Article

J. Braz. Chem. Soc., Vol. 23, No. 5, 951-957, 2012.
Printed in Brazil - ©2012 Sociedade Brasileira de Química
0103 - 5053 $6.00+0.00

Effect of Fluorination Treatment on Electrochemical Properties of $M1Ni_{3.5}Co_{0.6}Mn_{0.4}Al_{0.5}$ Hydrogen Storage Alloy

Hongxia Huang*,[a] and Kelong Huang[b]

[a]*College of Chemistry and Bioengineering, Guilin University of Technology, 541004 Guilin, PR China*

[b]*College of Chemistry and Chemical Engineering, Central South University, 410083 Changsha, PR China*

A influência do tratamento de superfície por soluções de NH_4F, LiF e LiF contendo KBH_4 na estrutura e nas propriedades electroquímicas da liga de armazenamento de hidrogênio $M1Ni_{3.5}Co_{0.6}Mn_{0.4}Al_{0.5}$ (onde M1 indica metal misto) é investigada. O tratamento de fluoração melhora as performances electroquímicas da liga $M1Ni_{3.5}Co_{0.6}Mn_{0.4}Al_{0.5}$. A capacidade de descarga máxima (C_{max}) aumenta de 314,8 para 325,7 (NH_4F), 326,5 (LIF) e 316,4 mAh g^{-1} (LiF+KBH_4). Após 60 ciclos, a taxa de retenção de capacidade aumenta de 83,5 para 84,8% (NH_4F), 89,5% (LIF) e 93,9% (LiF+KBH_4). Os resultados de polarização linear e polarização anódica revelam que a densidade de corrente de troca (I_0) e a densidade de corrente limitante (I_L) aumentam após tratamento de fluoração, indicando uma melhora na cinética de absorção/dessorção de hidrogênio.

The influence of surface treatment by solutions of NH_4F, LiF and LiF containing KBH_4 on the structure and electrochemical properties of the $M1Ni_{3.5}Co_{0.6}Mn_{0.4}Al_{0.5}$ hydrogen storage alloy (in which M1 denotes mischmetal) is investigated. The fluorination treatment improves the electrochemical performances of the $M1Ni_{3.5}Co_{0.6}Mn_{0.4}Al_{0.5}$ alloy. The maximum discharge capacity (C_{max}) increases from 314.8 to 325.7 (NH_4F), 326.5 (LiF) and 316.4 mAh g^{-1} (LiF+KBH_4). After 60 cycles, the capacity retention rate increases from 83.5 to 84.8% (NH_4F), 89.5% (LiF) and 93.9% (LiF+KBH_4). The results of the linear polarization and anodic polarization reveal that the exchange current density (I_0) and the limiting current density (I_L) increase after fluorination treatment, indicating an improvement of the kinetics of the hydrogen absorption/desorption.

Keywords: hydrogen storage alloys, $LaNi_5$-based electrode hydrides, fluorination treatment, electrochemical properties

Introduction

Metal hydrade/nickel (MH/Ni) batteries have been widely used due to their high energy density, durability to over charge/discharge and environmental friendliness.[1] The commercial AB_5-type and AB_2-type alloy electrodes can not meet the demand of the powder battery due to their intrinsical drawbacks.[2] In order to exploit new-type hydrogen storage alloys with high discharge capacity, good cycle stability and excellent kinetics performance, many approaches have been extensively studied, including substitution of alloy elements,[3-5] surface treatment,[6-9] composite alloys,[10,11] powder sieving,[12] and control of the charge input.[13] Among the above methods, fluorination treatment has shown great advantages in improving the hydriding performance of the alloy in a gas-solid system such as ease of activation, strong resistance against air or gaseous impurities, long storability in air or water, and non-pyrophoricity.[14] It is well-known that electrochemical properties are not only related to bulk compositions, but also to surface conditions for the formation of H atoms and the chemical absorption take place on the surface of alloy particles.[8] Therefore, it is expected that fluorination treatment of the sample may lead to obtain an alloy with high discharge capacity, excellent kinetic performance and good cycle stability.

Zhao *et al.*[8] reported that the discharge capacity, potential plateau and high rate dischargeability (HRD) of the $MmNi_{3.8}Co_{0.75}Mn_{0.4}Al_{0.2}$ (Mm = Ce-rich mischmetal) alloy were improved after treatment using the solution of HF and KF with a little addition of KBH_4. Liu and Suda[15,16] found the initial activation characteristics at low temperatures for Mg_2Ni and $MgLa_{1-x}Ni_x$ (x = 0.4-0.7) alloys enhanced by fluorination treatment. Xiao *et al.*[17] investigated the influence of the surface

*e-mail: hhxhunan@yahoo.com.cn

treatment by KBH_4 solution, alkaline solution and alkaline solution containing KBH_4 on the surface structure and electrochemical properties of the $La_{0.7}Mg_{0.3}Ni_{2.4}Co_{0.6}$ and confirmed that the alloy electrode treated by alkaline solution containing KBH_4 showed the best overall electrochemical properties. Kim *et al.*[18] claimed that the durability of the Mg_2Ni electrode markedly increased and a high discharge capability was obtained after fluorination treatment.

Though the discharge capacity of AB_5-type alloy electrodes is improved to some extent, it still cannot meet the demand of the powder battery. Surface modification is an effective method to enhance the overall characteristics of AB_5-type alloy. In order to improve the electrochemical properties, especially the discharge capacity and the kinetic performance of AB_5-type alloy, the effect of surface treatment by using different fluorine-containing aqueous solution on microstructure and electrochemical properties of the $M1Ni_{3.5}Co_{0.6}Mn_{0.4}Al_{0.5}$ alloy was systematically studied in this study.

Experimental

Preparation of alloys and electrodes

The $M1Ni_{3.5}Co_{0.6}Mn_{0.4}Al_{0.5}$ alloy (M1 consists of 37.7% La, 38.9% Ce, 6.3% Pr and 17.1% Nd) was prepared by induction melting under argon atmosphere. The alloy ingot was mechanically crushed to powders and then treated by immersion in the following three kinds of fluorine-containing aqueous solution (1) NH_4F, (2) LiF and (3) LiF+KBH_4 for 20 min and then ultrasonic for 2 h. The alloy powder was centrifuged and thoroughly washed with oxygen-free distilled water for several times to remove the soluble ions, and then kept at 90 °C in vacuum for 12 h.

The test electrodes were prepared by cold pressing a mixture of 0.10 g alloy powders with 0.20 g carbonyl nickel powders into a pellet of 10 mm in diameter under a pressure of 10 MPa and then pressed at 20 MPa between two pieces of foam nickel.

Characterization of alloys

The crystal structures of the alloys were identified by powder X-ray diffractometry (XRD) (Japan D/max 2550 VB+18 kV diffractometer) using CuK_α radiation (λ = 1.54178 Å).

Electrochemical charge/discharge test

The electrodes were soaked in 6 mol L^{-1} of KOH solution for 4 h before electrochemical measurements. The charge/discharge tests were performed by Land 5.3 B Battery Test instrument in half-cell consisting of working electrode, $Ni(OH)_2$/NiOOH counter electrode and 6 mol L^{-1} of KOH aqueous as electrolyte. The working electrodes were charged at current density of 100 mA g^{-1} for 6 h followed by 5 min resting time, and then discharged at the current density of 50 mA g^{-1} to the cut-off potential of 1.0 V.

During cyclic voltammograms (CV), linear polarization (LP), anodic polarization (AP), potentiodynamic polarization and electrochemical impedance spectra (EIS) tests, Hg/HgO electrode was used as reference electrode. PARSTAT 2273 advanced electrochemical system was used for potentiodynamic polarization measurement (scanning rate of 0.1 mV s^{-1}, potential range of –1.0 - –0.2 V *vs.* Hg/HgO), CV (scanning rate of 1 mV s^{-1}, potential range of –1.2 - –0.2 V *vs.* Hg/HgO), linear polarization (scanning rate of 0.1 mV s^{-1}, –5 - 5 mV *vs.* open circuit potential, 50% depth of discharge (DOD)), anodic polarization (0.5 mV s^{-1}, 0 - 500 mV *vs.* open circuit potential, 50% DOD) and EIS (amplitude of 5 mV, frequency range of 10^3 - 10^{-3} Hz, 50% DOD).

Results and Discussion

XRD analysis

Figure 1 shows the XRD patterns of the original and treated $M1Ni_{3.5}Co_{0.6}Mn_{0.4}Al_{0.5}$ alloys. It can be seen that all the alloys exhibit the diffraction peaks corresponding to the $LaNi_5$ phase with the $CaCu_5$-type hexagonal structure,[8] indicating that the crystal structure of the alloy is not affected by the surface treatments. The diffraction peaks become sharper after fluorination treatment, implying in a better crystallization of the $LaNi_5$ phase due to the

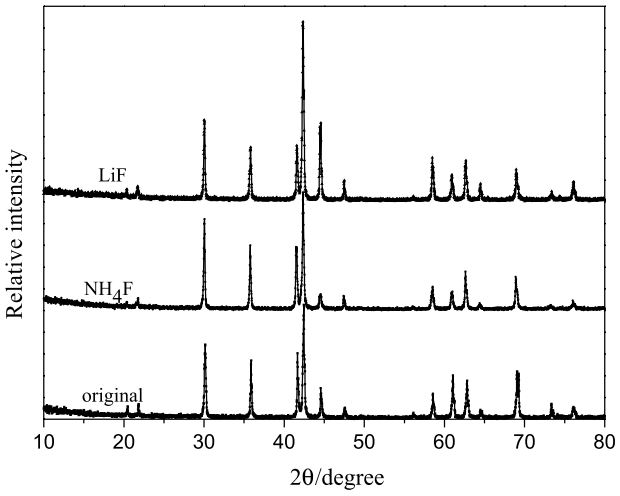

Figure 1. XRD patterns of the original and the treated $M1Ni_{3.5}Co_{0.6}Mn_{0.4}Al_{0.5}$ alloys.

composition homogenization caused by the surface treatment.[2] The lattice parameters of the $LaNi_5$ phase calculated by XRD Rietveld analysis are listed in Table 1.

Table 1. The lattice parameters of the original and the treated $M1Ni_{3.5}Co_{0.6}Mn_{0.4}Al_{0.5}$ alloys

Samples	Phase	Lattice parameter / Å		Cell volume / Å^3	*c*/*a*
		a	*c*		
Original	$LaNi_5$	5.063	4.063	90.20	0.802
NH_4F	$LaNi_5$	5.010	4.061	88.31	0.811
LiF	$LaNi_5$	5.002	4.070	88.21	0.814

As can be seen, the lattice parameters *a* and *c* and thus the cell volume of the $LaNi_5$ phase changed after the treatment. The variation of cell volume and lattice parameters for $LaNi_5$ phase may be related to the surface treatment by different fluorine-containing aqueous solution.

Discharge properties

Figure 2 shows the cycle number dependence of the discharge capacity of the original and the treated $M1Ni_{3.5}Co_{0.6}Mn_{0.4}Al_{0.5}$ alloy electrodes.

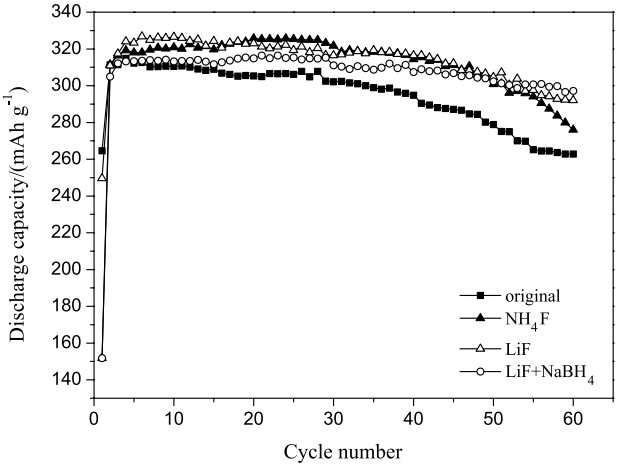

Figure 2. The relationship between the cycle number and the discharge capacity of the original and the treated $M1Ni_{3.5}Co_{0.6}Mn_{0.4}Al_{0.5}$ alloy electrodes.

The maximum discharge capacity (C_{max}) and the discharge potential at 50% DOD are presented in Table 2. It can be seen that C_{max} for the alloy electrodes increases from 314.8 to 325.7 (NH_4F), 326.5 (LiF) and 316.4 mAh g^{-1} (LiF+KBH_4). It is shown that the addition of KBH_4 exerts a negative effect on the discharge capacity, and the result agrees with the study of Xiao *et al.*[17] The decisive factors of the discharge capability of the alloy are the phase structure, surface state, grain size, composition homogeneity and interstitial dimensions.[19] The increment of discharge capacity by fluorination treatment is attributed to the following three reasons: (*i*) fluorination treatment can peeled-off the La_2O_3-type passive film covering on the surface of particles and form a porous, water insoluble fresh fluoride top-layer overlapping a metallic Ni-enriched substrate. The fluorinated surface has a strong affinity for hydrogen uptake and provides channel-like free paths for H atoms to easily diffuse from the surface to the bulk,[15] which is advantageous for the discharge capacity of the treated alloy electrodes. (*ii*) During fluorination treatment, the formed metallic Ni acts as not only a site for easy hydrogen penetration but also as a catalyst for the dissociation of molecular hydrogen to atomic hydrogen. (*iii*) The fluorination treatment minimizes the particle size, which increases the contact probability of electrode with the electrolyte and much fresh surface or interface is formed, consequently, induces the better discharge capacity of alloy electrode.

The root cause of leading to battery lose efficacy is on negative electrode rather than on positive electrode. The failure of battery is characterized by the decay of the discharge capacity. The fundamental factors leading to the deterioration of discharge capacity of the hydrogen storage alloy electrodes are the pulverization of the alloy particles during consecutive hydrogenation/dehydrogenation and the oxidation/corrosion of alloy components in alkaline electrolyte.[2] The capacity retention rate (S_n) used to characterize the cycle stability can be calculated by the following expression:

$$S_n\,(\%) = C_n / C_{max} \times 100 \qquad (1)$$

where the C_n is the discharge capacity at cycle number n and C_{max} is the maximum discharge capacity. The capacity retention rate of the alloy electrodes are shown in Table 2. After 60 cycles, the capacity retention rate increases from 83.5 to 84.8 (NH_4F), 89.5 (LiF) and 93.9% (LiF+KBH_4). The fact confirms that the surface treatment improves the cycle durability of the alloy electrode. The reason for the improved cycle stability after fluorination treatment can be explained by a relatively lower cell volume that changes during hydriding/dehydriding. The literature indicated that the degradation of the discharge capacity of alloy electrode is related to the unit cell anisotropy, which can be expressed by the lattice parameter ratio: *c*/*a*.[20] The higher anisotropy factor *c*/*a* will induce a smaller change of the lattice during hydrogenation, and in consequence the better degradation resistance. As shown in Table 1, the anisotropy factor of the $LaNi_5$ phase increased after fluorination treatment, which is responsible for the

Table 2. Summary of electrochemical properties of the original and the treated $M1Ni_{3.5}Co_{0.6}Mn_{0.4}Al_{0.5}$ alloy electrodes

Samples	C_{max} / (mAh g^{-1})	Discharge potential at 50% DOD / V	S_{40} / %	S_{60} / %	R_p / mΩ	I_0 / (mA g^{-1})	I_L / (mA g^{-1})
Original	314.8	1.3221	93.6	83.5	333.3	77.0	443.4
NH_4F	325.7	1.3129	96.5	84.8	125.2	205.2	483.5
LiF	326.5	1.3349	96.9	89.5	147.5	174.2	589.9
LiF+KBH_4	316.4	1.3230	97.1	93.9	151.9	169.1	523.9

improvement of the cyclic stability of the treated alloy electrodes. Among the treated alloy electrodes, the sample treated by LiF+KBH_4 solution exhibits the highest cycle stability. Before charge/discharging cycles, a metal-hydride form and the anti-oxidation ability is reinforced due to the addition of KBH_4.[8] During charge/discharge cycles, the hydrogen storage alloy is continuously protected by the metal-hydrides, which is responsible for the improved cycle performance of the alloy electrode.

Cyclic voltammograms (CV)

The CV curves of the original and the treated $M1Ni_{3.5}Co_{0.6}Mn_{0.4}Al_{0.5}$ alloy electrodes are depicted in Figure 3.

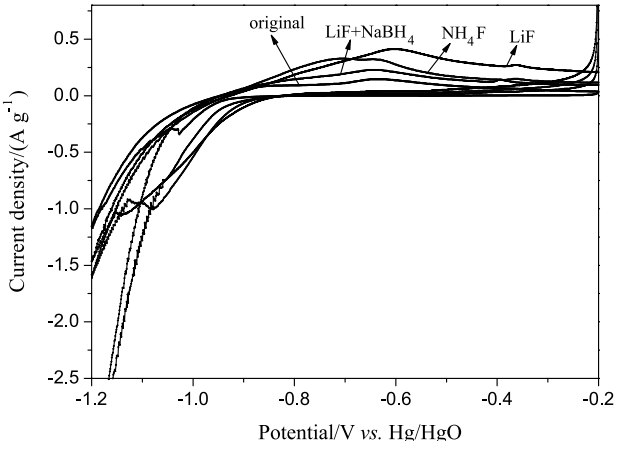

Figure 3. The CV curves of the original and the treated $M1Ni_{3.5}Co_{0.6}Mn_{0.4}Al_{0.5}$ alloy electrodes at scan rate 1 mV s^{-1}.

The anodic peak at around –0.6 - –0.7 V *vs*. Hg/HgO is attributed to the oxidation of hydrogen absorbed in the alloy according to the following equation:[21]

$$MH_n + n\ OH^- \rightarrow M + n\ H_2O + n\ e^- \quad (2)$$

The oxidation current density corresponds to the hydrogen desorption from the interior to the surface of the alloy particles.[22] The height of the oxidation/reduction peak can be used to evaluate the kinetic activity of the hydride electrode.[23] As can be seen from Figure 3, the oxidation peak current of the treated alloy electrodes is increased compared to that of original alloy, which is ascribable to the formation of the metallic Ni and the increase of the specific surface area as a result of the reduction of the particle size after fluorination treatment. Tliha *et al*.[24] ascribed the peak area to the capacity of hydrogen desorption, the larger peak area indicates the higher discharge capacity. The anodic area of the treated alloy electrodes is larger than the original one, indicating fluorination treatment improves the hydrogen storage capacity of the alloy electrode, and the variation of peak area is in agreement with that of the maximum discharge capacity. The cathodic peak at around –1.05 - –1.10 V *vs*. Hg/HgO is attributed to the hydriding reaction according to above equation at opposite side.

Linear polarization (LP)

Figure 4 presents the linear polarization curves of the original and the treated $M1Ni_{3.5}Co_{0.6}Mn_{0.4}Al_{0.5}$ alloy electrodes. Obviously, there is a linear dependence of polarization current and overpotential. Exchange current density I_o is one of the parameters describing the kinetic characteristics of electrodes and used to judge the speed of charge transfer on the surface of electrodes.[25] The polarization resistance R_p can be determined from the ration of the overpotential (η) to the current density (I_d) and the exchange current density I_0 is obtained from the following formula:

$$I_0 = \frac{RTI_d}{F\eta} \quad (3)$$

where I_d is the applied current density, R is the gas constant, T is the absolute temperature, F is the Faraday constant, and η is the overpotential of the electrochemical reaction for the hydrogen storage alloys. The calculated values of I_0 and R_p are tabulated in Table 2. It can be seen that R_p decreases and I_0 increases after fluorination treatment,

which means that the electrochemical reaction ability is improved due to the elimination of surface oxide layers covering on the surface of particles and the formation of a metallic Ni-enriched substrate.

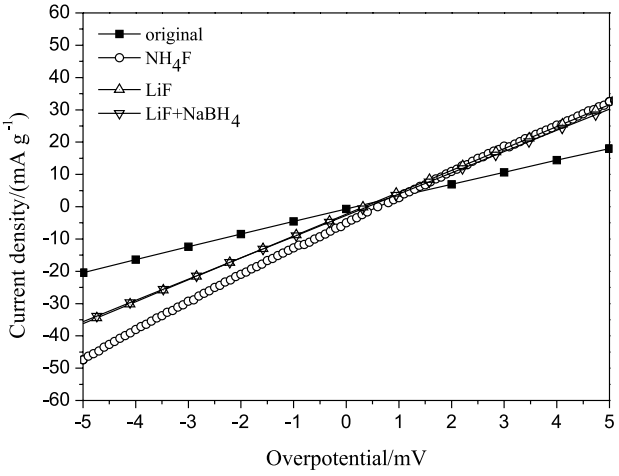

Figure 4. Linear polarization curves of the original and the treated $M1Ni_{3.5}Co_{0.6}Mn_{0.4}Al_{0.5}$ alloy electrodes at 50% DOD (scanning rate: 0.1 mV s^{-1}).

Anodic polarization (AP)

Figure 5 exhibits the anodic polarization curves of the original and treated $M1Ni_{3.5}Co_{0.6}Mn_{0.4}Al_{0.5}$ alloy electrodes. It can be seen the anodic current density increases first and then reaches a maximum with increasing overpotential, which is defined as the limiting current density (I_L). The limiting current density indicates that an oxidation reaction takes place on the surface of the alloy electrode and the oxidation product prevents further penetration of the H atoms.[26] The limiting current density I_L is mainly controlled by the hydrogen diffusion in the bulk of the alloy.

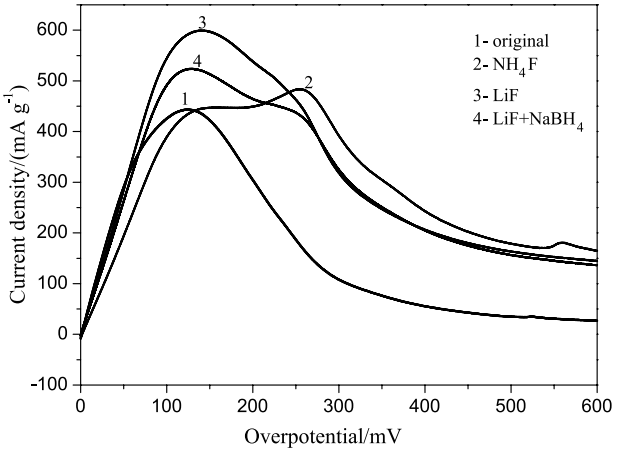

Figure 5. Anodic polarization curves of the original and the treated $M1Ni_{3.5}Co_{0.6}Mn_{0.4}Al_{0.5}$ alloy electrodes at 50% DOD at scan rate 0.5 mV s^{-1}.

The larger is the limiting current density I_L, the higher is the rate of the hydrogen diffusion inside the alloy. The I_L values of the alloy electrodes obtained from Figure 5 are also summarized in Table 2. After surface treatment, the I_L of the treated alloy electrodes is higher than that of the original alloy electrode, and the electrode treated by LiF has the highest limiting current density. The fluorination treatment increases the limiting current density of the alloy electrode, which suggests that the hydrogen diffusivity in the alloy improved.

Potentiodynamic polarization

There should be two factors caused the degradation of the discharge capacity of the hydrogen storage alloy electrodes, one is the pulverization of the alloys during consecutive charge/discharge cycles, and the other is the oxidation and the corrosion of the alloy components in the alkaline electrolyte. Many efforts have been made to improve the anti-corrosion performance of alloy electrodes in alkaline solution, because the corrosion is a barrier to its practical application. Figure 6 shows the potentiodynamic polarization curves of the original and the treated $M1Ni_{3.5}Co_{0.6}Mn_{0.4}Al_{0.5}$ alloy electrodes, and the value of corrosion voltage (E_{corr}) obtained through Tafel fitting are indicated. It is noteworthy that the variation of the corrosion voltage (E_{corr}) is not completely consistent with the cycle stability shown in Table 2. It reveals that the inhibition of metal corrosion is not always the main factor for the improvement of cycle performance of alloy electrode. As can been seen in Table 1, the anisotropy factor (*c*/*a*) of the $LaNi_5$ phase increased after fluorination treatment, indicating a better pulverization resistance of the treated alloy electrodes, which is responsible for the improvement of the cycle durability of the alloy electrodes.

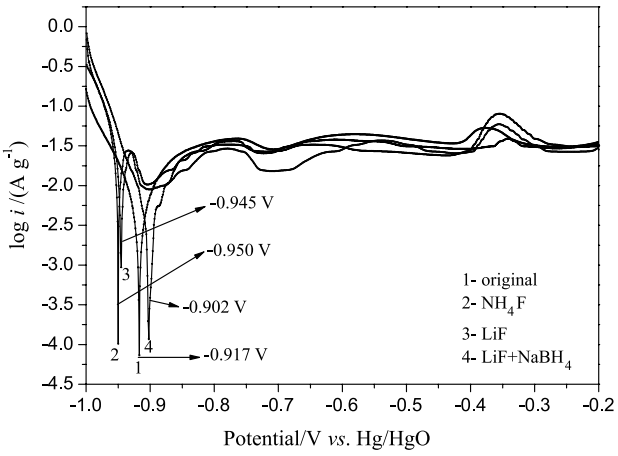

Figure 6. The potentiodynamic polarization curves of the original and the treated $M1Ni_{3.5}Co_{0.6}Mn_{0.4}Al_{0.5}$ alloy electrodes (scanning rate: 0.1 mV s^{-1}).

Electrochemical impedance spectra (EIS) tests

Figure 7 shows the electrochemical impedance spectra (EIS) of the original and treated $M1Ni_{3.5}Co_{0.6}Mn_{0.4}Al_{0.5}$ alloy electrodes. It can be seen that each spectrum consists of a small semicircle in the high-frequency region and a large semicircle in the low-frequency region followed by a straight line. Kuriyama *et al.*[27] ascribed the high-frequency semicircle to the contact resistance between the current collector and the alloy pellet, the middle-frequency semicircle to the charge-transfer resistance and the straight line at low-frequency to the Warburg impedance. It is clear that the semicircle at low frequency for the treated alloy electrodes is smaller than that for original sample. This illustrates that the electrochemical reaction resistance R_{ct} of the treated alloy electrode decreases after fluorination treatment, thus the treated alloy electrodes exhibit the higher discharge capacity in the charge/discharge cycles.

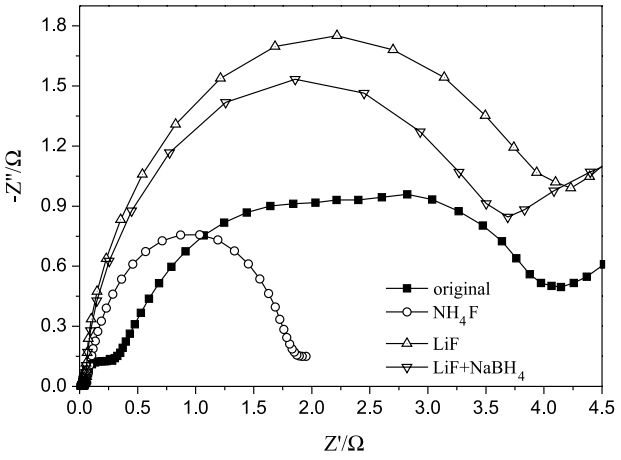

Figure 7. The electrochemical impedance spectra (EIS) of the original and treated $M1Ni_{3.5}Co_{0.6}Mn_{0.4}Al_{0.5}$ alloy electrodes at 50% DOD.

Conclusions

Fluorination treatment of the $M1Ni_{3.5}Co_{0.6}Mn_{0.4}Al_{0.5}$ hydrogen storage alloy is carried out by using different fluorine-containing aqueous solution. The electrochemical properties of the original and the treated alloy electrodes are studied. The maximum discharge capacity for the alloy electrodes increases from 314.8 to 325.7 (NH_4F), 326.5 (LiF) and 316.4 mAh g^{-1} (LiF+KBH_4), respectively. After 60 cycles, the capacity retention rate increases from 83.5 to 84.8 (NH_4F), 89.5 (LiF) and 93.9% (LiF+KBH_4). Moreover, the results for the electrochemical kinetic measurement indicate that the electrochemical kinetic performance of the alloy electrode is improved after fluorination treatment, which is mainly ascribed to the formation of Ni-rich layer.

Acknowledgments

This work was supported by the scientific research project of Guangxi Educational Department. The authors wish to express their thanks to the colleagues of Institute of Functional Materials and Chemistry of Central South University for their help.

References

1. Zhang, Z.; Han, S. M.; Li, Y.; Jing, T. F.; *J. Alloys Compd.* **2007**, *431*, 208.
2. Miao, H.; Pan, H. G.; Zhang, S. C.; Chen N.; Li, R.; Gao, M. X.; *Int. J. Hydrogen Energy* **2007**, *32*, 3387.
3. Liu, Y. F; Pan, H. G; Gao, M. X; Miao, H.; Lei, Y. Q.; Wang, Q. D.; *Int. J. Hydrogen Energy* **2008**, *33*, 124.
4. Miao, H.; Liu, Y. F.; Lin, Y.; Zhu, D.; Jiang, L.; Pan, H. G.; *Int. J. Hydrogen Energy* **2008**, *33*, 134.
5. Li, Y.; Han, D.; Han, S. M.; Zhu, X. L.; *Int. J. Hydrogen Energy* **2009**, *34*, 1399.
6. Chen, W. X; Xu, Z. D.; Tu, J. P.; Li, H. Y.; Yuan, J.; Chen, S.; *Int. J. Hydrogen Energy* **2001**, *26*, 675.
7. Li, Y.; Jiang, L. J.; Huang, Z.; Zhan, F.; Wu, B. R.; Xia, Z. H.; *J. Alloys Compd.* **1999**, *293-295*, 687.
8. Zhao, X. Y.; Ding, Y.; Yang, M.; Ma, L. Q.; *Int. J. Hydrogen Energy* **2008**, *33*, 81.
9. Park, H. Y.; Cho, W. I.; Cho, B. W.; Lee, S. R.; Yun, K. S.; *J. Power Sources* **2001**, *92*, 149.
10. Wang, Y.; Qiao, S. Z.; Wang, X.; *Int. J. Hydrogen Energy* **2008**, *33*, 1023.
11. Chu, H. L.; Qiu, S. J.; Sun, L. X.; Zhang, Y.; Xu, F.; Zhu, M.; Hu, W. Y.; *Int. J. Hydrogen Energy* **2008**, *33*, 755.
12. Rongeat, C.; Grosjean, M-H.; Ruggeri, S.; Dehmas, M.; Bourlot, S.; Marcotte, S.; Roué, L.; *J. Power Sources* **2006**, *158*, 747.
13. Ruggeri, S.; Roue, L.; *J. Power Sources* **2003**, *117*, 260.
14. Liu, F.-J.; Sandrock, G. D.; Suda, S.; *J. Alloys Compd.* **1992**, *190*, 57.
15. Liu, F.-J.; Suda, S.; *J. Alloys Compd.* **1996**, *232*, 212.
16. Liu, F.-J.; Suda, S.; *J. Alloys Compd.* **1995**, *231*, 696.
17. Xiao, L. L.; Wang, Y. J.; Liu, Y.; Song, D. W.; Jiao, L. F.; Yuan, H. T.; *Int. J. Hydrogen Energy* **2008**, *33*, 3925.
18. Kim, J. S.; Lee, C. R.; Choi, J. W.; Kang, S. G.; *J. Powder Sources* **2002**, *104*, 201.
19. Zhang, Y. H.; Li, B. W.; Ren, H. P.; Wu, Z. W.; Yin, Cai.; Wang, X. L.; *Mater. Chem. Phys.* **2007**, *105*, 86.
20. Ma, S.; Gao, M. X.; Li, R.; Pan, H. G.; Lei, Y. Q.; *J. Alloys Compd.* **2008**, *457*, 457.
21. Chen, Y.; *Catal. Today* **1998**, *44*, 3.
22. Liu, Y. F.; Pan, H. G.; Gao, M.; *J. Alloys Compd.* **2004**, *373*, 304.

23. Guo, Z. P.; Huang, Z. G.; Konstantinov, K.; Liu, H. K.; Dou, S. X.; *Int. J. Hydrogen Energy* **2006**, *31*, 2032.
24. Tliha, M.; Mathlouthi, H.; Khaldi, C.; Lamloumia, J.; Percheronguegan, A.; *J. Power Sources* **2006**, *160*, 10.
25. Notten, P. H. L.; Hokkeling, P.; *J. Electrochem. Soc.* **1991**, *138*, 1877.
26. Niu, H.; Northwood, D. O.; *Int. J. Hydrogen Energy* **2002**, *27*, 69.
27. Kuriyama, N.; Sakai, T.; Miyamura, H.; Uehara, I.; Ishikawa, H.; Iwasaki, T.; *J. Alloys Compd.* **1993**, *202*, 183.

Submitted: September 9, 2011
Published online: April 24, 2012